



# Tropical Journal of Natural Product Research


Available online at <https://www.tjnpr.org>*Original Research Article*

## Flavonoids Exhibit Potential Antagonistic Activity Against Platelet-Activating Factor (PAF) Receptor

Noraziah Nordin<sup>a\*</sup>, Adib A. Abdullah<sup>b</sup>, Mohd F. A. Ghani<sup>a</sup><sup>a</sup>Department of Basic Medical Sciences I, Faculty of Medicine & Health Sciences, Universiti Sains Islam Malaysia, 71800, Nilai, Negeri Sembilan, Malaysia<sup>b</sup>Department of Pharmaceutical Chemistry, Faculty of Pharmacy, University Malaya, 50603, Kuala Lumpur, Malaysia

## ARTICLE INFO

## ABSTRACT

*Article history:*

Received 17 May 2022

Revised 18 October 2022

Accepted 19 October 2022

Published online 01 November 2022

**Copyright:** © 2022 Nordin *et al.* This is an open-access article distributed under the terms of the [Creative Commons Attribution License](https://creativecommons.org/licenses/by/4.0/), which permits unrestricted use, distribution, and reproduction in any medium, provided the original author and source are credited.

The platelet-activating factor receptor (PAFR) has been a therapeutic target for platelet-activating factor (PAF)-mediated diseases. The pathophysiological condition is triggered by the interaction of PAF agonist. The discovery of PAF antagonists from natural flavonoids could be promising candidates for treating PAF-mediated diseases. Flavonoids that exist in most edible plants possess good health benefits to the human body. The study aimed to investigate the ability of three flavonoids (apigenin, galangin and fisetin) for molecular docking and dynamic simulations into PAFR protein. The PAFR-flavonoid complex binding affinities and interactions were assessed through molecular docking and dynamic simulations. Results found that all flavonoids significantly have a good binding affinity, ranging from - 9.1 to - 8.9 kcalmol<sup>-1</sup>. The stability of these flavonoids was also achieved in a 30 ns simulation. Four critical residues were detected in all PAFR-flavonoids complexes (Phe97, Phe98, Thr101 and Leu279) from the analysis of MMGBSA binding free energy. Interactions of van der Waals and electrostatic were seen by individual key residues of PAFR for the free energy contribution of ligands binding. All flavonoids showed promising anti-PAF candidate to be developed in the future.

**Keywords:** Methylglyoxal, AGEs, Advanced glycation end products, Glutathione, Magnesium, Ubiquinone.

### Introduction

The platelet-activating factor receptor (PAFR) is a G-protein receptor with seven trans membrane domains.<sup>1</sup> It has been the therapeutic target for PAF-mediated diseases for many years.<sup>2</sup> The PAFR is capable of binding to its natural ligand, PAF, and stimulates some signalling mechanisms in the body.<sup>1</sup> The complex of PAF-PAFR triggers inflammatory pathways which induce pathological responses, such as cancer, chronic obstructive pulmonary disease (COPD), asthma, allergic disorders, neurodegenerative disorders and immune suppression.<sup>2</sup> PAF receptor is identified in several organ tissues, including the brain, platelets, leucocytes and muscles.<sup>2,3</sup> These distributions throughout the body cause so many implications of PAF binding into PAFR. To inhibit the pathological conditions due to PAF-PAFR interaction, PAF antagonists have been developed, which also have the capability to bind with PAFR. The action of PAF antagonists may competitively or non-competitively displace PAF agonists from PAFR active site.<sup>4</sup> To date, various molecules exhibit PAFR antagonistic activity potentials, such as structurally related synthetic PAF derivatives, synthetic compounds without structural similarity to PAF, metal complexes, and natural products.<sup>5</sup> The implication of the natural PAF antagonists is to inhibit and reduce all undesirable reactions in the body.<sup>6</sup> Among PAF antagonists reported are including ginkgolide B, kadsurenone and glitoxins.<sup>7</sup>

\*Corresponding author. E mail: [noraziahnordin@usim.edu.my](mailto:noraziahnordin@usim.edu.my)

Tel: +606-7985002

**Citation:** Nordin N, Abdullah AA, Ghani MFA. Flavonoids Exhibit Potential Antagonistic Activity Against Platelet-Activating Factor (PAF) Receptor. Trop J Nat Prod Res. 2022; 6(10):1626-1631. <http://www.doi.org/10.26538/tjnpr/v6i10.11>

Official Journal of Natural Product Research Group, Faculty of Pharmacy, University of Benin, Benin City, Nigeria.

Therefore, the potential of natural product compounds as PAF antagonists are tested in the flavonoids which contain a very large class of polyphenolic compounds in the plant kingdom.<sup>8</sup> Flavonoids consisted of the 15-carbon skeleton which forms two phenyl rings, A and B connected by a heterocyclic 4H-pyrane ring named C.<sup>8</sup> Three tested flavonoids (apigenin, galangin and fisetin) in this study were variance in the number of the hydroxyl group and the position on the basic flavone structure. These flavonoids were also reported in several biological activities such as antiviral,<sup>9-10</sup> anticancer,<sup>11-13</sup> antiplatelet,<sup>14-15</sup> anti-inflammatory,<sup>16-18</sup> and antioxidant.<sup>19-21</sup> A recent study found that apigenin, galangin and fisetin interacted with cancer-related proteins at low binding affinities in molecular docking analysis.<sup>22</sup> Some key features have been identified in the PAFR binding site in the in-silico modelling studies, which consisted of a bipolarized cylinder and shorter domain.<sup>23</sup> A large lipophilic binding pocket and a hydrogen bond donor that can interact with either a carbonyl or oxygen atom of the flavonoids is hoped to anticipate a better interaction towards antagonistic reaction.<sup>2</sup> This study aimed to generate a comprehensive conformation of the PAFR-flavonoid complex according to their stability and understanding of the dynamic behaviour of the final complex to improve the further process of the drug discovery process.

### Materials and Methods

#### Preparation of Ligand Structural Files

The structures of three selected flavonoids were retrieved from the PubChem database (<http://pubchem.ncbi.nlm.nih.gov/>) (Figure 1). The BIOVIA Discovery Studio 2017 R2 was used to build the three-dimensional ligand structures. Meanwhile, the minimization of each structure was done using the Hyperchem Pro 6.0 software to form the lowest energy conformations.

#### Preparation of Protein Structural File

The protein structure of PAFR was obtained from the RCSB Protein Data Bank (PDB ID: 5ZKP).<sup>24</sup> Heteroatoms and water molecules from

the PAFR structure were removed using Discovery studio Visualizer v3.1 (Accelrys Inc. San Diego, CA, USA). Besides, both hydrogen and nonpolar hydrogen atoms were added and merged to the PAFR protein, respectively. Gasteiger charges were then added to the protein preparation before assigning AutoDock type atoms to the PAFR protein.

#### Molecular Docking Simulation

AutoDock Vina software was used for all docking simulations in this study.<sup>25</sup> The flavonoids were positioned at the binding site of PAFR. Before site-directed docking by all flavonoids, blind docking was performed into PAFR using SR 27417 and cedrol, which were PAFR antagonists. The docking simulation at the identified binding site was done with exhaustiveness set to 100 and repeated 10 times to determine the docking conformation. A receptor grid file was produced with a grid box dimension of  $20 \times 20 \times 20$  Å on the x, y and z axes, with coordinates X = 31.978, Y = -3.429, and Z = 8.69. The flavonoids-PAFR binding interactions were assessed using the Discovery Studio Visualizer.

#### Molecular Dynamics (MD) Simulation

Molecular dynamics (MD) was conducted based of the selection from the best-docked conformers to evaluate the binding stability of the flavonoid-PAFR complex. The topology of PAFR protein was done using the Amber ff14SB force field,<sup>26</sup> in which hydrogen atoms were added to the defined topology of PAFR. Meanwhile, all ligands (flavonoids and cedrol) were determined using the general AMBER force field (GAFF)<sup>27</sup> with the AM1-BCC charge model.<sup>28</sup> The complex of PAFR-flavonoid was solvated with TIP3P water model<sup>29</sup> in a rectangular box of 10 Å margin. The system was neutralized by adding sodium and chloride, accordingly. The preparation steps of those inputs were carried out using the AmberTools18 software suite,<sup>30</sup> particularly the Antechamber package<sup>31</sup> and tLEaP programs. Six phases of the simulation were conducted, including positional-restraint minimization, full minimization, positional-restraint heating, positional-restraint density, equilibration and production. In the positional-restraint phase, the PAFR-flavonoid complex's heavy atoms were weakly restrained with a  $10 \text{ kcalmol}^{-1}$  A-3 harmonic force constant. This minimization phase was done using the L-BFGS algorithm<sup>32-33</sup> as well as the full minimization until the system locally converged at  $1 \text{ kJmol}^{-1}$  energy tolerance. The positional-restraint heating phase was done in a canonical ensemble (NVT) for 50 ps from 0 to 300 K in a gradual 2-K increment. The positional-restraint density phase was carried out in an isothermal-isobaric ensemble (NPT) for 50 ps at 300 K. The two equilibration and production phases were performed in an isothermal-isobaric ensemble (NPT) at 300 K for 1 ns and 30 ns, respectively. The temperature of the NVT ensemble was maintained at 300 K using the

Langevin thermostat<sup>34-35</sup> with a friction coefficient of  $1 \text{ ps}^{-1}$ . Meanwhile, the temperature of the NPT ensemble was maintained as in the NVT ensemble, and the pressure was sustained at 1 bar using Monte Carlo barostat.<sup>36-37</sup> All phases in the MD simulation were run using OpenMM version 7.3<sup>38</sup> incorporated with the NVIDIA GTX Titan X card. A periodic boundary fashion was set for the simulation process in a Langevin dynamics<sup>34-35</sup> with a 2 fs time step. The SHAKE/SETTLE algorithm was used for constraining the covalent bonds between the heavy atom and hydrogen atom.<sup>39-40</sup> The non-bonded (first type of interaction) and electrostatic interactions were assessed using the particle-mesh Ewald method<sup>41</sup> with a cut-off of 10 Å to limit the calculation of direct space sum. Meanwhile, the interaction of van der Waals (the second type of the non-bonded interaction), was truncated at 10 Å.

#### Post-MD Analysis

The evaluation of the binding properties of the ligands was conducted using a 30 ns production trajectory. MD simulation stability and the ligand-binding stability were obtained via calculation of the root mean square deviation (RMSD) of the protein and ligand, respectively. The calculation of hydrogen bonding in flavonoids and PAFR were done using the CPPTRAJ program,<sup>42</sup> which is comprised of AmberTools18.

#### Calculation of Free Energy of Binding

Molecular mechanics energies incorporated with generalized Born and surface area continuum solvation (MMGBSA) were used to determine the free energy of binding. All free energies were calculated using 100 trajectory frames throughout the production trajectory. The process was reported in a python script, MMPBSA.py<sup>43</sup>, using the AmberTools18.

## Results and Discussion

#### Docked Flavonoids into PAFR

This study was conducted to examine the molecular docking between flavonoids with PAFR protein. The results presented in Table 1 show that all studied flavonoids had better binding affinities, ranging from -9.1 to -8.9  $\text{kcalmol}^{-1}$ , compared with cedrol (-8.1  $\text{kcalmol}^{-1}$ ) as a positive PAF antagonist drug. Apigenin and galangin exhibited the same binding affinity of -9.1  $\text{kcalmol}^{-1}$ . However, apigenin interacted with PAFR through two different intermolecular interactions, which are hydrogen bonds and hydrophobic interaction. Interesting to note that three critical residues formed  $\pi$ -interactions between the ring structures of flavonoids with Trp73, Phe97 and Leu279 of PAFR protein (Figures 2 and 3). The same residues of PAFR have also interacted with cedrol, hydrophobically. Fisetin was seen to have the highest H-bonds formation as compared to apigenin and galangin (Table 1).

**Table 1:** Docking results illustrating the binding affinities and interaction profile of standard agonist and antagonist of PAF and flavonoids with PAFR.

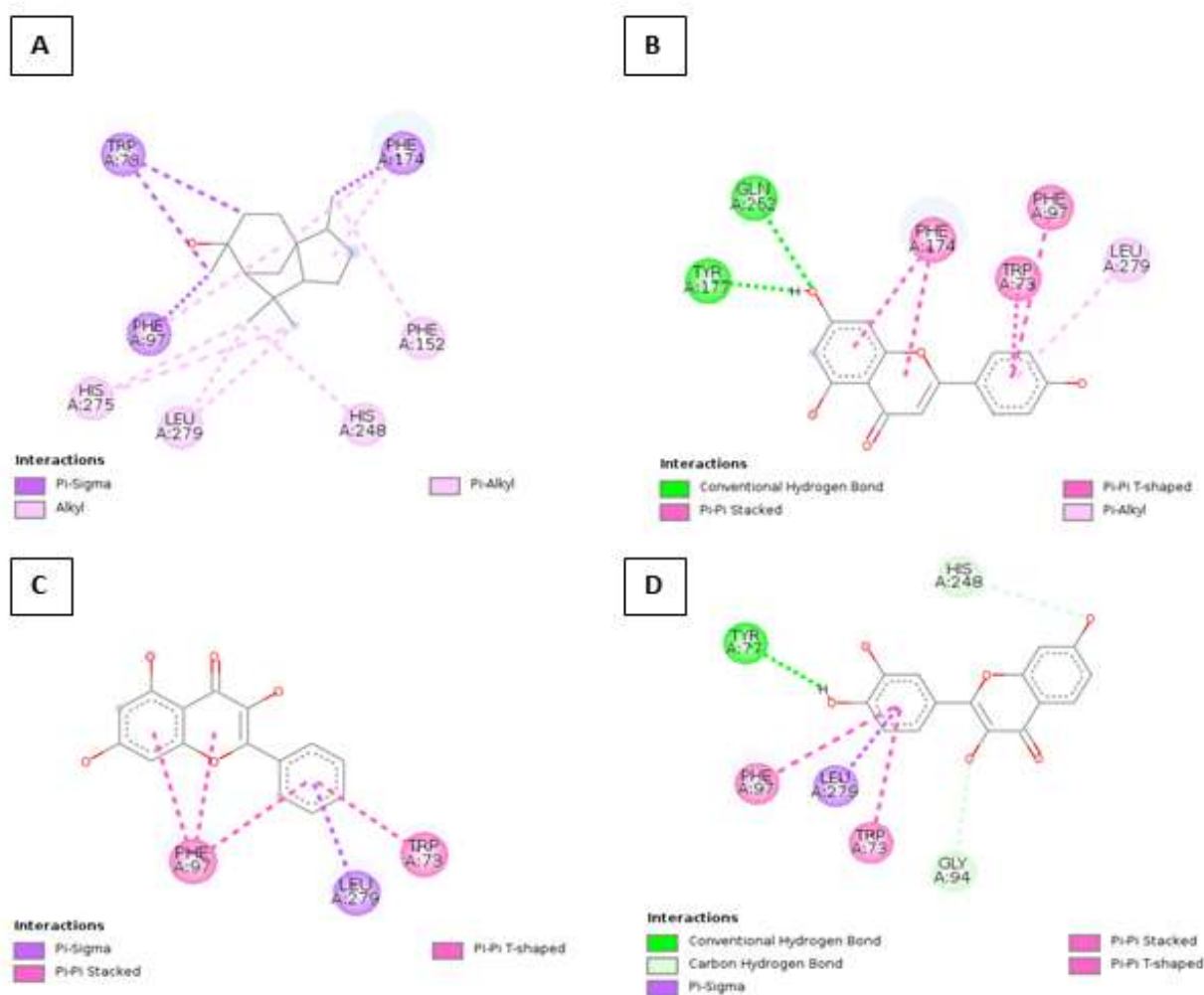
Ligand	Binding Affinity ( $\text{kcalmol}^{-1}$ )	Hydrogen Bonding	Hydrophobic Interaction	Electrostatic Interaction
SR 27417 (re-docked antagonist)	-10.6	Tyr77, Phe174	Trp73, Phe97, Phe98, Tyr102, Phe152, His188, Ile191, His248, Leu279, Leu282	-
Cedrol (antagonist)	-8.1	-	Trp73, Phe97, Phe152, Phe174, His248, His275, Leu279	-
PAF (agonist)	-7.9	Tyr151, Asp156, His176, His188	Phe18, Tyr22, Trp77, Leu279	His188
Apigenin	-9.1	Tyr177, Gln252	Trp73, Phe97, Phe174, Leu279	-
Galangin	-9.1	-	Trp73, Phe97, Leu279	-
Fisetin	-8.9	Tyr77, Gly94, His248	Trp73, Phe97, Leu279	-

Cys: Cysteine, Asp: Aspartate, Glu: Glutamate, Phe: Phenylalanine, Gly: Glycine, His: Histidine, Ile: Isoleucine, Leu: Leucine, Gln: Glutamine, Arg: Arginine, Thr: Threonine, Trp: Tryptophan, Tyr: Tyrosine.



**Figure 1:** Structures of flavonoids

This could be due to the presence of more hydroxyl groups in its structure. In contrast,  $\pi$ - $\pi$  interactions were detected in all rings A, B and C of apigenin and galangin, but not fisetin (Figure 2), which contributed to the higher binding affinity of apigenin and galangin. As shown in Table 1, the binding affinity of PAF agonist was slightly weaker than antagonist ligands. As the PAFR could be activated or deactivated,<sup>44</sup> both agonist and antagonist ligands interact at different residues of the PAFR binding pocket. All flavonoids acted antagonistically at the same binding pocket with PAFR, which is similar to cedrol as an antagonist drug (Figure 4). In addition, interaction with Phe97 at helix III and helix IV position of PAFR, which is found in all flavonoids, suggested the blocking conformation towards the inactive mode of PAFR.<sup>45</sup> The antagonistic action of these three flavonoids (apigenin, galangin and fisetin) were expected to compete with PAF agonist with better binding affinity against PAFR.

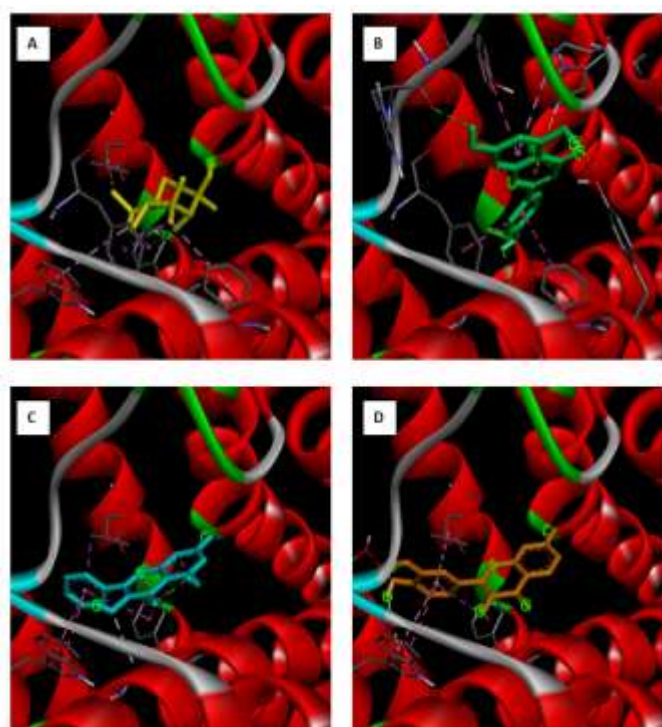


**Figure 2:** Two-dimensional illustration of binding interaction of the flavonoids and cedrol with the residues within the binding site of PAFR. a) Cedrol b) Apigenin, c) Galangin, d) Fisetin.

**Table 2:** Analysis of MD simulation on PAFR binding site in complex with standards and flavonoids

Ligand	RMSD (Å)	van der Waals	Electrostatic	Total	Key Residue
SR 27417 (antagonist)	1.52 ± 0.27	-69.3849 ± 4.1718	-12.9869 ± 4.1690	-56.4263 ± 6.3791	Arg14, Tyr22, Trp73, Phe97, Phe98, Phe152, Phe174, Gln252, Leu279
Cedrol (antagonist)	6.24 ± 0.52	-33.8335 ± 2.4504	-4.7380 ± 3.0725	-29.3495 ± 2.8356	Phe97, Phe98, Phe174  Phe97, Phe98, Thr101, Phe152, Phe174, Tyr177,
PAF (agonist)	5.57 ± 0.44	-80.1787 ± 3.4786	-79.6490 ± 7.4553	-79.9716 ± 5.2763	His188, Ile191, His248, Gln252, Trp255, Leu279, Leu282
Apigenin	3.68 ± 0.23	-31.9933 ± 3.2409	-32.5584 ± 3.7755	-33.5873 ± 2.7083	Phe97, Phe98, Thr101, Glu175, Leu279
Galangin	4.20 ± 0.38	-33.6591 ± 2.9131	-14.1740 ± 3.9503	-26.6665 ± 3.2034	Phe97, Phe98, Thr101, Leu279, Leu282
Fisetin	3.34 ± 0.27	-35.3665 ± 2.9542	-36.1582 ± 14.4099	-35.3989 ± 8.2078	Phe97, Phe98, Thr101, Phe174, Glu175, His188, Gln252, Leu279

All values represent means ± SD

**Figure 3:** Three-dimensional illustration of binding interaction of the flavonoids and cedrol with the residues within the binding site of PAFR. a) Cedrol, b) Apigenin, c) Galangin, d) Fisetin.**Figure 4:** Three-dimensional illustration of all flavonoids overlaid with cedrol in PAFR.

Furthermore, as the agonist induces the mitogen-activated protein kinase (MAPK) pathway,<sup>2</sup> these flavonoids could inhibit the MAPK cascade, leading to anti-inflammatory responses. The preliminary findings of docking were further validated with MD simulation on the binding interaction and stability of the flavonoid/PAFR complex.

#### Analysis of RMSD in Molecular Dynamic Simulation of PAFR in Complex with Flavonoids

Further validation of PAF-flavonoid docking interactions was conducted via MD simulation. Besides, the complex formation of protein-ligand was also examined. The MD trajectory analysis involved in RMSD calculation are shown in Table 2 and Figure 5. Results show that re-docking with SR-27417 into PAFR exhibits a slightly RMSD deviation from its position of 1.52 ± 0.27 Å. All tested flavonoids exhibited the RMSD value from 3.34 to 4.20 Å. The deviation could be due to the adaptation of these small ligands (Figure 5) to the dynamic of the binding pocket. This corroborated the initial conformation as predicted by the docking study.

#### Analysis of MMGBSA Binding Free Energy

The estimation of binding free energy of the PAFR-flavonoid complex was analysed via MMGBSA calculation. The total free energies of binding ( $\Delta GTOT$ ) are tabulated in Table 2. Based on the findings, the  $\Delta GTOT$  values of flavonoids ranged from - 35.39 to - 26.66 kcalmol<sup>-1</sup>. Fisetin and apigenin exhibited higher total free energies of binding with - 35.39 and - 33.5873 kcalmol<sup>-1</sup>, respectively, compared with an antagonist PAF (PAFR-cedrol) of - 29.3495 kcalmol<sup>-1</sup>. The interactions from MMGBSA analysis found that van der Waals interaction contributed equally to all flavonoids. In contrast, an electrostatic interaction was detected to be far different in binding free energy value for galangin with -14.1740 ± 3.9503 kcalmol<sup>-1</sup>. The PAFR-fisetin complex appeared to be the most stable, with the lowest free energy of binding of - 35.39 kcalmol<sup>-1</sup> in 30 ns MD simulation. This flavonoid also exhibited more key residues than apigenin and galangin. Among the key residues from fisetin are Phe97, Phe98, Thr101, Phe174, Glu175, His188, Gln252 and Leu279 (Table 2). However, four residues of PAFR (Phe97, Phe98, Thr101 and Leu279) were found to have interacted in all flavonoids (apigenin, galangin and fisetin). Of these four residues, Phe98 and Thr101 were not detected to be bound with all ligands in the initial molecular docking. Similarly, Trp73 which was found in the interaction of protein-ligand in the docking study, was not observed after MD simulation. The validation by the MD simulation suggested that apigenin, galangin and fisetin stabilize the binding site of hydrophobic and van der Waals interaction. The findings establish the binding pose obtained from the docking study of all studied flavonoids. Specific contribution per residue in the ligand-binding will give a better view of an understanding of PAFR-flavonoid interaction.

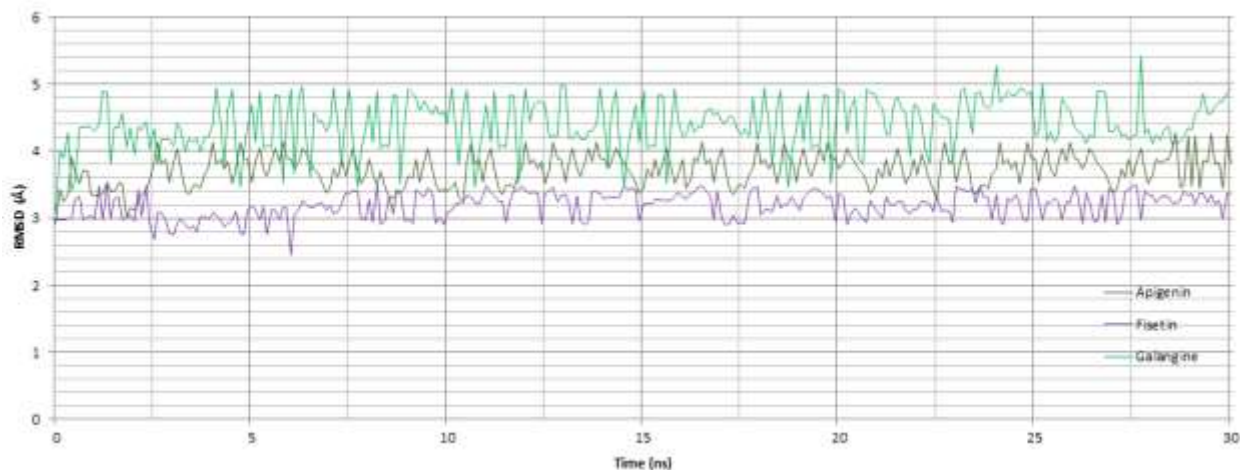


**Figure 5:** RMSD of PAFR docked with apigenin, galangin and fisetin in 30 ns simulation.

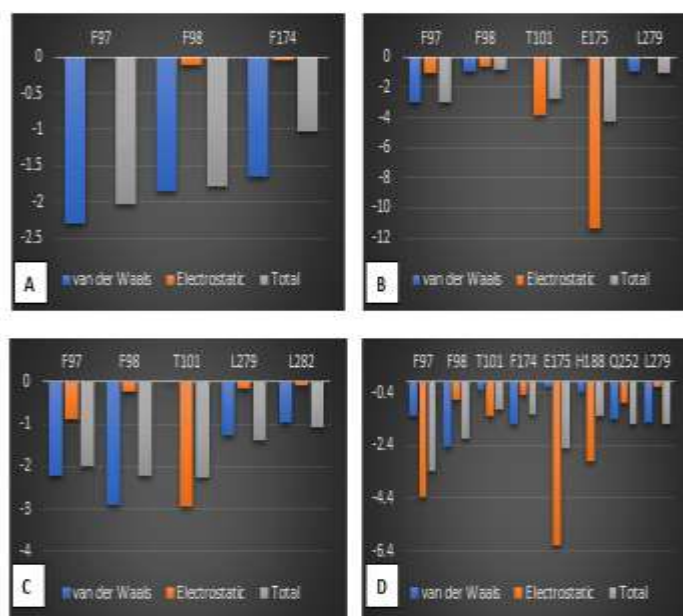


**Figure 6:** MMGBSA binding energy decomposition (per residue). Per residue-free energy of binding with negative contributions of van der Waals and electrostatic interactions with (a) Cedrol, (b) Apigenin, (c) Galangin and (d) Fisetin. F: Phenylalanine, T: Threonine, E: Glutamate, L: Leucine, H: Histidine, Q: Glutamine

#### Contribution of Individual Residue in Ligand Binding

The contribution of individual residue in the ligand-binding against PAFR is illustrated in Figure 6. An F97 (Phe97) residue contributed to the highest van der Waals interaction, nearly  $-5.0 \text{ kcalmol}^{-1}$  in apigenin, compared with galangin and fisetin. However, the lowest total per residue-free energy contribution for apigenin was seen at E175 (Glu175), which was given by electrostatic interaction. Similarly, fisetin exhibits the lowest E175 (Glu175) binding energy contribution of  $-6.4 \text{ kcalmol}^{-1}$  for electrostatic interaction among other residues. Nevertheless, the less total binding energy per residue was contributed more from F97 (Phe97). All key residues were anticipated to be equally contributed to the per residue-free energy of binding either by van der Waals or electrostatic interactions in all PAFR-flavonoid complexes

#### Conclusion

The tested flavonoids and the PAFR have been investigated for the docking and MD simulations. All flavonoids demonstrated better

docking binding with PAFR in its active site. Furthermore, the validation of each ligand interaction through MD simulation confirmed the docking protocol. This suggests that apigenin, galangin and fisetin have a promising effect on PAF antagonists. In the future, these findings could be used for the biological evaluation of PAF-mediated diseases for exploring strategies concerning these flavonoids.

#### Conflict of Interest

The authors declare no conflict of interest.

#### Authors' Declaration

The authors hereby declare that the work presented in this article is original and that any liability for claims relating to the content of this article will be borne by them.

#### Acknowledgements

We would like to thank Universiti Sains Islam Malaysia under Grant Agreement No (PPP/FPSK/0118/051000/14918) for their financial supports to conduct this study.

#### References

- Shukla SD, Fairbairn RL, Gell DA, Latham RD, Sohal SS, Walters EH, O'Toole RF. An antagonist of the platelet-activating factor receptor inhibits adherence of both nontypeable *Haemophilus influenzae* and *Streptococcus pneumoniae* to cultured human bronchial epithelial cells exposed to cigarette smoke Int J Chron Obstruct Pulmon Dis. 2016; 11:1647–1655.
- Hyland IK, O'Toole RF, Smith JA, Bissember AC. Progress in the Development of Platelet-Activating Factor Receptor (PAFR) Antagonists and Applications in the Treatment of Inflammatory Diseases. ChemMedChem. 2018; 13(18):1873-84.
- Fukunaga A, Khaskhely NM, Sreevidya CS, Byrne SN, Ullrich SE. Dermal dendritic cells, and not Langerhans cells, play an essential role in inducing an immune response. J Immunol. 2008; 180(5):3057-3064.
- Tsoupras AB, Iatrou C, Frangia C, Demopoulos CA. The implication of platelet activating factor in cancer growth and metastasis: potent beneficial role of PAF-inhibitors and antioxidants. Infect Disord Drug Targets. 2009; 9(4):390-399.
- Shukla SD. Platelet-activating factor receptor and signal transduction mechanisms. The FASEB J. 1992; 6(6):2296-2301.
- Lordan R, Tsoupras A, Zabetakis I, Demopoulos CA. Forty years since the structural elucidation of platelet-activating factor

- (PAF): historical, current, and future research perspectives. *Molecules*. 2019; 24(4414):1-32.
7. Whittaker M. Overview: PAF Receptor Antagonists: Recent Advances. *Expert Opin Ther Pat*. 1992; 2(5):583-623.
  8. Raffa D, Maggio B, Raimondi MV, Plescia F, Daidone G. Recent discoveries of anticancer flavonoids. *Eur J Med Chem*. 2017; 142:213-228.
  9. Hakobyan A, Arabyan E, Avetisyan A, Abroyan L, Hakobyan L, Zakaryan H. Apigenin inhibits African swine fever virus infection *in vitro*. *Arch Virol*. 2016; 161(12):3445-3453.
  10. Lani R, Hassandarvish P, Shu MH, Phoon WH, Chu JJ, Higgs S, Vanlandingham D, Bakar SA, Zandi K. Antiviral activity of selected flavonoids against Chikungunya virus. *Antivir Res*. 2016; 133:50-61.
  11. Madunić J, Madunić IV, Gajski G, Popić J, Garaj-Vrhovac V. Apigenin: A dietary flavonoid with diverse anticancer properties. *Cancer Lett*. 2018; 413:11-22.
  12. Kumar R and Tikku AB. Galangin induces cell death by modulating the expression of glyoxalase-1 and Nrf-2 in HeLa cells. *Chem-Biol Interact*. 2018; 279:1-9.
  13. Rengarajan T and Yaacob NS. The flavonoid fisetin as an anticancer agent targeting the growth signaling pathways. *Eur J Pharmacol*. 2016; 789:8-16.
  14. Karličková J, Říha M., Filipický T, Macáková K, Hrdina R, Mladěnka P. Antiplatelet effects of flavonoids mediated by inhibition of arachidonic acid-based pathway. *Planta Med*. 2016; 82(01/02):76-83.
  15. Lee JH, Kim M, Chang KH, Hong CY, Na CS, Dong MS, Lee D, Lee MY. Antiplatelet effects of *Rhus verniciflua* Stokes heartwood and its active constituents—fisetin, butein, and sulfuretin—in rats. *J Med Food*. 2015; 18(1):21-30.
  16. Ginwala R, Bhavsar R, Chigbu DG, Jain P, Khan ZK. Potential role of flavonoids in treating chronic inflammatory diseases with a special focus on the anti-inflammatory activity of apigenin. *Antioxidants*. 2019; 8(35):1-28.
  17. Lee HN, Shin SA, Choo GS, Kim HJ, Park YS, Kim BS, Kim SK, Cho SD, Nam JS, Choi CS, Che JH. Anti-inflammatory effect of quercetin and galangin in LPS-stimulated RAW264. Macrophages and DNCB-induced atopic dermatitis animal models. *Int J Mol Med*. 2018; 41(2):888-898.
  18. Pal HC, Pearlman RL, Afaq F. Fisetin and its role in chronic diseases. *Anti-inflammatory Nutraceuticals and Chronic Diseases*. 2016; 213-244.
  19. Zhang H, Zheng W, Feng X, Yang F, Qin H, Wu S, Hou DX, Chen J. Nrf2–ARE signaling acts as master pathway for the cellular antioxidant activity of fisetin. *Molecules*. 2019; 24(708):2-16.
  20. Devadoss D, Ramar M, Chinnasamy A. Galangin, a dietary flavonol inhibits tumor initiation during experimental pulmonary tumorigenesis by modulating xenobiotic enzymes and antioxidant status. *Arch Pharm Res*. 2018; 41(3):265-275.
  21. Telange DR, Patil AT, Pethe AM, Fegade H, Anand S, Dave VS. Formulation and characterization of an apigenin-phospholipid phytosome (APLC) for improved solubility, *in vivo* bioavailability, and antioxidant potential. *Eur J Pharm Sci*. 2017; 108:36-49.
  22. Ghani MFA, Hamid NA, Nordin N. Flavonoids Docked into Several Target Proteins Associated with Cancer: A Molecular Docking Study. *Trop J Nat Prod Res*. 2021; 5(12):2057-2062
  23. Benmehdi H, Lamouri A, Serradji N, Pallois F, Heymans F. Synthesis of New Trisubstituted 4-Aminopiperidines as PAF-Receptor Antagonists. *Eur J Org Chem*. 2008; 299-307.
  24. Cao C, Tan Q, Xu C, He L, Yang L, Zhou Y, Zhou Y, Qiao A, Lu M, Yi C, Han GW. Structural basis for signal recognition and transduction by platelet-activating-factor receptor. *Nat Struct Mol Biol*. 2018; 25(6):488-495.
  25. Jaghoori MM, Bleijlevens B, Olabarriaga SD. 1001 Ways to run AutoDock Vina for virtual screening. *J Comp-aided Mol Desgn*. 2016; 30(3):237-249.
  26. Maier JA, Martinez C, Kasavajhala K, Wickstrom L, Hauser KE, Simmerling C. ff14SB: improving the accuracy of protein side chain and backbone parameters from ff99SB. *J Chem Theory Comput*. 2015; 11(8):3696-3713.
  27. Wang J, Wolf RM, Caldwell JW, Kollman PA, Case DA. Development and testing of a general amber force field. *J Comput Chem*. 2004; 25(9):1157-1174.
  28. Jakalian A, Jack DB, Bayly CI. Fast, efficient generation of high-quality atomic charges. AM1-BCC model: II. Parameterization and validation. *J Comput Chem*. 2002; 23(16):1623-1641.
  29. Jorgensen WL, Chandrasekhar J, Madura JD, Impey RW, Klein ML. Comparison of simple potential functions for simulating liquid water. *Chem Phys*. 1983; 79(2):926-935.
  30. Case DA, Ben-Shalom IY, Brozell SR, Cerutti DS, Cheatham III TE, Cruzeiro VW, Darden TA, Duke RE, Ghoreishi D, Gilson MK, Gohlke H. AMBER. University of California, San Francisco; 2018.
  31. Wang J, Wang W, Kollman PA, Case DA. Antechamber: an accessory software package for molecular mechanical calculations. *J Am Chem Soc*. 2001; 222:U403.
  32. Liu DC, Nocedal J. On the limited memory BFGS method for large scale optimization. *Math Program*. 1989; 45(1):503-528.
  33. Nocedal J. Updating quasi-Newton matrices with limited storage. *Math Comput*. 1980; 35(151):773-782.
  34. Loncharich RJ, Brooks BR, Pastor RW. Langevin dynamics of peptides: The frictional dependence of isomerization rates of N-acetylalanyl-N'-methylamide. *Biopolymers: Original Research on Biomolecules*. 1992; 32(5):523-535.
  35. Pastor RW, Brooks BR, Szabo A. An analysis of the accuracy of Langevin and molecular dynamics algorithms. *Mol Phys*. 1988; 65(6):1409-1419.
  36. Åqvist J, Wennerström P, Nervall M, Bjelic S, Brandsdal BO. Molecular dynamics simulations of water and biomolecules with a Monte Carlo constant pressure algorithm. *Chem Phys Lett*. 2004; 384(4-6):288-294.
  37. Chow KH, Ferguson DM. Isothermal-isobaric molecular dynamics simulations with Monte Carlo volume sampling. *Comput Phys Commun*. 1995; 91(1-3):283-289.
  38. Eastman P, Swails J, Chodera JD, McGibbon RT, Zhao Y, Beauchamp KA, Wang LP, Simmonett AC, Harrigan MP, Stern CD, Wiewiora RP. OpenMM 7: Rapid development of high-performance algorithms for molecular dynamics. *PLoS Comput Biol*. 2017; 13(7):e1005659.
  39. Miyamoto S and Kollman PA. Settle: An analytical version of the SHAKE and RATTLE algorithm for rigid water models. *J Comput Chem*. 1992; 13(8):952-962.
  40. Ryckaert JP, Ciccotti G, Berendsen HJ. Numerical integration of the cartesian equations of motion of a system with constraints: molecular dynamics of n-alkanes. *J Comput Phys*. 1977; 23(3):327-341.
  41. Darden T, York D, Pedersen L. Particle mesh Ewald: An N·log(N) method for Ewald sums in large systems. *Chem Phys*. 1993; 98(12):10089-10092.
  42. Roe DR, Cheatham III TE. PTRAJ and CPPTRAJ: software for processing and analysis of molecular dynamics trajectory data. *J Chem Theory Comput*. 2013; 9(7):3084-3095.
  43. Miller III BR, McGee Jr TD, Swails JM, Homeyer N, Gohlke H, Roitberg AE. MMPBSA. py: an efficient program for end-state free energy calculations. *J Chem Theory Comput*. 2012; 8(9):3314-3321.
  44. Cao C, Tan Q, Xu C, He L, Yang L, Zhou Y, Zhou Y, Qiao A, Lu M, Yi C, Han GW. Structural basis for signal recognition and transduction by platelet-activating-factor receptor. *Nat Struct Mol Biol*. 2018; 25(6):488-495.
  45. Jantan I, Jalil J, Abdul Warif NM. Platelet-activating factor (PAF) antagonistic activities of compounds isolated from *Guttiferae* species. *Pharm Biol*. 2001b; 39(4):243-246